Hydrogen Desorption Properties of Nanocrystalline MgH$_2$-10 wt.% ZrB$_2$ Composite Prepared by Mechanical Alloying

M. Maddah[1], M. Rajabi[1], S. M. Rabiee[1]

Abstract

Storage of hydrogen is one of the key challenges in developing hydrogen economy. Magnesium hydride (MgH$_2$) is an attractive candidate for solid-state hydrogen storage for on-board applications. In this study, 10 wt.% ZrB$_2$ was co-milled with magnesium hydride at different milling times to produce nanocrystalline composite powder. The effect of milling time and additive on the hydrogen desorption properties of obtained powder was evaluated by thermal analyzer method and compared with pure MgH$_2$. The phase constituents of powder particles were characterized by X-ray diffractometry method. The grain size and lattice strain of β-MgH$_2$ phase were estimated from the broadening of XRD peaks using Williamson–Hall method. The size and morphological changes of powder particles upon mechanical alloying were studied by scanning electron microscopy. XRD analysis showed that the mechanically activated magnesium hydride consisted of β-MgH$_2$, γ-MgH$_2$ and small amount of MgO. It is shown that the addition of ZrB$_2$ to magnesium hydride yields a finer particle size. The thermal analyses results showed that the addition of ZrB$_2$ particle to magnesium hydride and mechanical alloying for 30 h reduced the dehydrogenation temperature of magnesium hydride from 319 °C to 308 °C. This can be attributed to the particle size reduction of magnesium hydride.

Keywords: Hydrogen desorption; magnesium hydride; Mechanical alloying; Nanocrystalline composite

1. Introduction

Hydrogen is an ideal energy carrier and renewable fuel which is considered for future transport, such as automotive applications. The relatively advanced storage methods such as high-pressure gas or liquid cannot fulfill future storage goals [1, 2]. Magnesium hydride is one of the attractive hydrogen storage materials because of its hydrogen storage capacity (7.6 wt %), low cost and light weight [1-3]. However, high hydrogen desorption temperature, relatively poor hydrogen absorption-desorption kinetics and a high reactivity toward air and oxygen limit the use of MgH$_2$ in practical applications [4-6].

Many efforts have focused on Mg-based hydrides in recent years to reduce the desorption temperature and to fasten the re/dehydrogenation reactions. These can be accomplished to some extent by changing the microstructure of the hydride by mechanical alloying which reduce the stability of the hydrides and also by using proper catalysts to improve the absorption/desorption kinetics [1].

Metal oxides are both catalysts and very efficient milling agents that can create defects in structure due to their ceramic nature and ability to produce small grain size defects [7]. Non-oxide ceramics such as SiC, TiB$_2$ and TiC facilitate the rupture of MgH$_2$ particles and consequently reduce the particle size and increase the specific surface area [7]. The influence of TiB$_2$ on hydrogen desorption of MgH$_2$ has been reported and maximum temperature decrease of hydride decomposition was found to be 60 °C [8]. Simchi et al. [9] have found that the addition of Nb$_2$O$_5$ to MgH$_2$ and affording mechanical alloying decreases desorption temperature to ~220 °C. Polanski et al. [10] have shown that the specific surface area of MgH$_2$ powder after milling with nanosized Cr$_2$O$_3$ decreases significantly as compared to the powder milled without catalyst. In this work, ZrB$_2$ powder was added to the magnesium hydride and the

1- Department of Mechanical Engineering, Babol Noshirvani University of Technology , P.O.Box 47148-71167, Shariati Street, Babol, Iran.

Corresponding author: M. Rajabi, Department of Mechanical Engineering, Babol Noshirvani University of Technology, P.O.Box 47148-71167, Shariati Street, Babol, Iran.
Email: m.rajabi@nit.ac.ir

mixture was mechanically alloyed for different times. The effect of additive on the dehydrogenation temperature was investigated and compared with pure magnesium hydride.

2. Experimental

Elemental powders of MgH_2 (98%, Merck) and ZrB_2 (90%, Sigma-Aldrich) were used as starting materials. Firstly, pure MgH_2 was mechanically milled for two different times (5 and 30 h) as the reference base. Secondly, MgH_2 powder was blended with 10 wt.% ZrB_2 and mechanical alloying was performed in a Retsch PM100 planetary ball mill at room temperature under a high purity argon atmosphere for 5 and 30 h. Ball to powder weight ratio of 20:1 was selected and rotation speed was adjusted to 400 rpm. Weighing, filling and handling of the powders were performed in a glove box under argon atmosphere.

The phase formation and variation of grain structure were investigated by X-ray diffraction method (X'Pert Pro MPD, PANalytical) with Cu-K_α radiation. The crystallite size and lattice strain of β-MgH_2 phase were estimated from the broadening of XRD peaks using Williamson–Hall method [9]. The size and morphological changes of powder particles upon mechanical alloying were studied by scanning electron microscopy (SEM, Philips XL30). The mean particle size of powders was measured using Clemex Vision image analyser on SEM images. The dehydrogenation properties were investigated with a simultaneous thermal analyzer (NETSCH STA 503) under argon atmosphere at a heating rate of 5 °C/min up to 500 °C.

3. Result and Discussion

Fig. 1 shows the XRD patterns of pure MgH2 powder at the selected milling times. The XRD peak of un-milled MgH_2 powder was included in the graph for comparison. As seen, with increasing of the milling time, all diffraction peaks of β-MgH_2 are broadened and decreased evidently due to the high-energy impact of the milling balls. After 5 h milling, the diffraction peaks corresponding to γ-MgH_2 are detected. Additionally, the appearance of
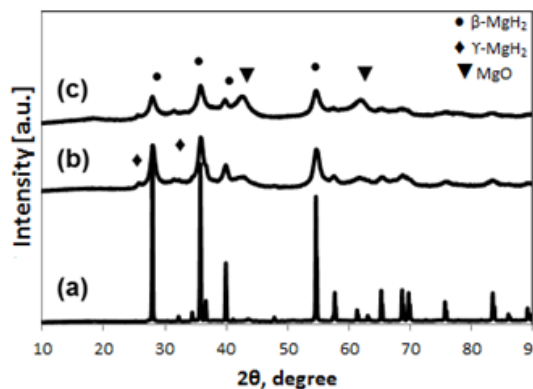

Fig. 1. X-ray diffraction patterns of pure MgH_2 powder at different milling times: (a) 0 h, (b) 5 h, and (c) 30 h.

XRD peaks of MgO determines the oxidation magnesium during the milling. The results obtained from XRD, SEM and STA are summarized in Table 1. As can be seen, the crystallite size is gradually decreased from 25 nm to 18 nm with increasing milling time from 5 h to 30 h. A significant particle size refinement is observed and after milling up to 30 h, the particle size reduced to about 1.6 μm. Here, no significant difference in the particle morphology is observed as the milling time increases from 5 h to 30 h (see Fig. 2).

Fig. 3 shows the effect of milling time on the dehydrogenation temperature of mechanically activated MgH_2. Each DTA curve contains two distinct endothermic peaks, which correspond to the hydrogen release reaction. The position of the first peak indicates the temperature at which the dehydrogenation reaction has the maximum rate and thus it is considered as the dehydrogenation temperature in this work. As seen, mechanical milling affects the dehydrogenation of MgH_2 and the lowest

Table 1. Average particle size (D), crystallite size (d), lattice strain (ε) and dehydrogenation temperature (T) of MgH_2 at different milling times

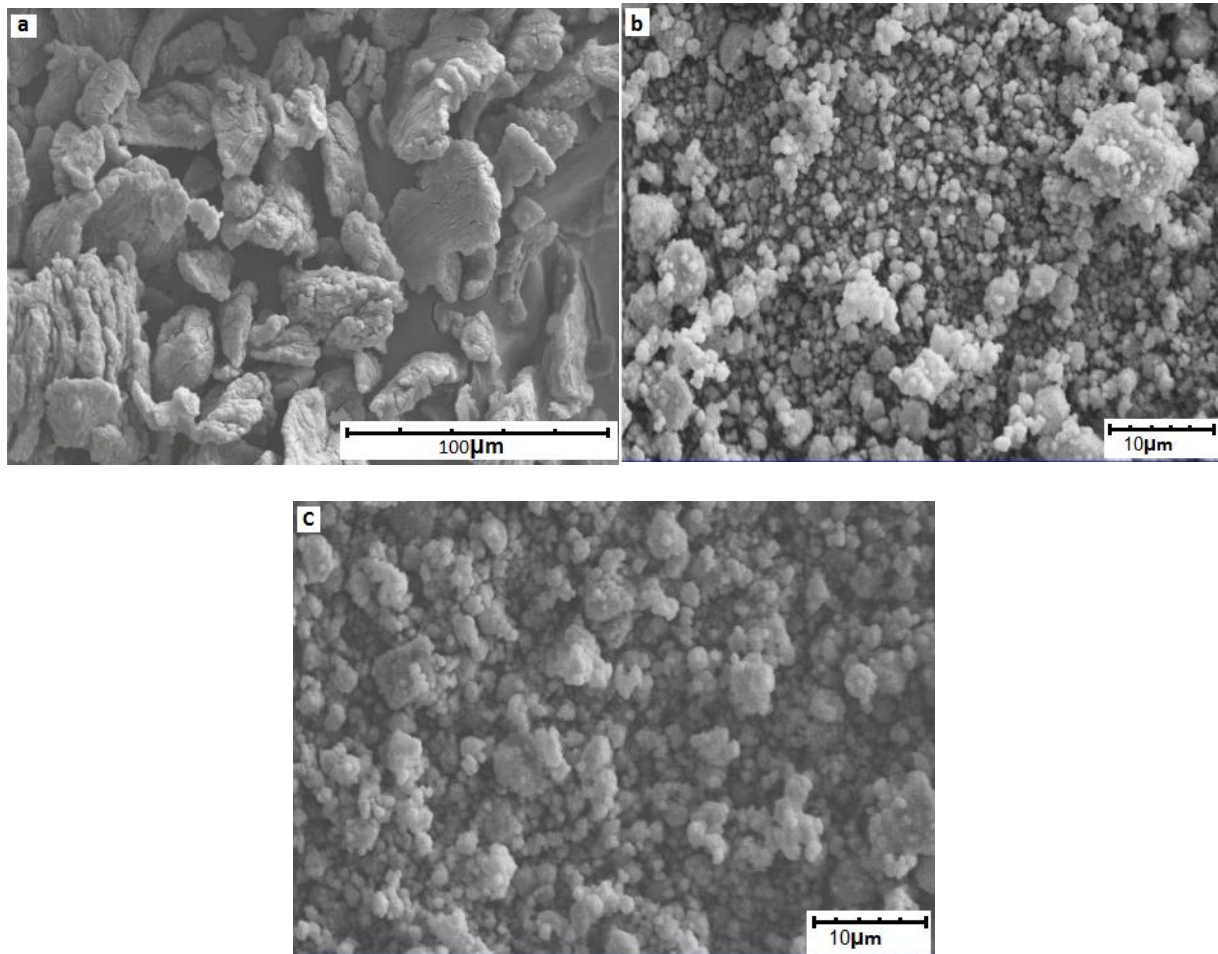| Time, h	Phase	D, μm	d, nm	ε, %	T, (°C)
0	β	30	60	0	421
5	β, γ, MgO	2.2	25	0.3	340
30	β, γ, MgO	1.6	18	0.7	319

Fig. 2. SEM micrographs of magnesium hydride powder for un-milled (a) and milled for 5 h (b) and 30 h (c).

desorption temperature was obtained at 319 °C which corresponds to 30 h milling. This temperature is about 100 °C lower than that of the as-received MgH_2. The results presented in Table 1 demonstrate that high-energy mechanical alloying affects the hydrogenation of MgH_2 in agreement with previous reports [10, 11]. The possible reasons include: (i) formation of metastable γ-MgH_2 phase, (ii)

Fig. 3. DTA curves of pure MgH_2 milled for different times.

significant refinement of powder particles, (iii) finer grain size and accumulation of lattice strain which affects the decomposition and diffusion. The metastable high-pressure orthorombic γ-MgH_2 phase, which has a lower desorption enthalpy and temperature [12], would affect the thermodynamics and kinetics of dehydrogenation process, so its formation decreases the hydrogen desorption temperature of MgH_2.
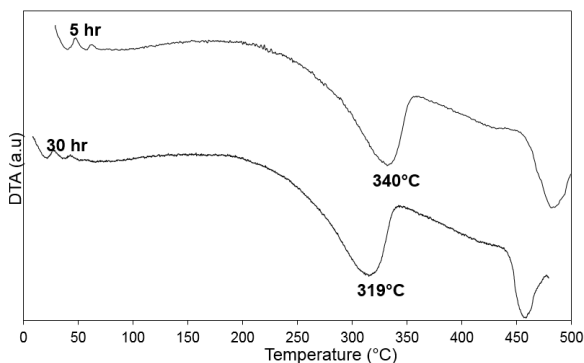
Since the diffusion of H-atoms in grain boundaries much faster than that of entire lattice, thereby, the grain refinement decreases the diffusion path and eventually affects the desorption kinetics. The high lattice strain also influences the hydrogenation, so that the minimum dehydrogenation temperature (319 °C) was obtained for the powder with d=18nm and ε=0.7%. Here, it should be mentioned that the formation of MgO may affect the dedydrogenation process. In fact, MgO acts as a barrier between the solid and gas phase by

limiting the diffusion of hydrogen atoms through its dense structure [9].

Fig. 4 shows the XRD patterns of MgH_2-10 wt.% ZrB_2 nanocrystalline composite produced by mechanical alloying at two different times. After 5 h milling, the diffraction peaks corresponding to β-MgH_2 and MgO are observed in the XRD pattern. The absence of ZrB_2 peaks in the XRD pattern is due to their low concentrations. With the milling time extended up to 30 h, the diffraction peaks corresponding to β-MgH_2 become broader and less intensity, while those corresponding to MgO intensify, showing the presence of higher amounts of this phase with increasing milling time. No new phase formation was noticed at this time. Fig. 5 shows the dehydrogenation of the composite material as a function of temperature for the two selected milling times. To compare the dehydrogenation behavior, the characteristics of the synthesized nanocrystalline composite powder at different milling times were
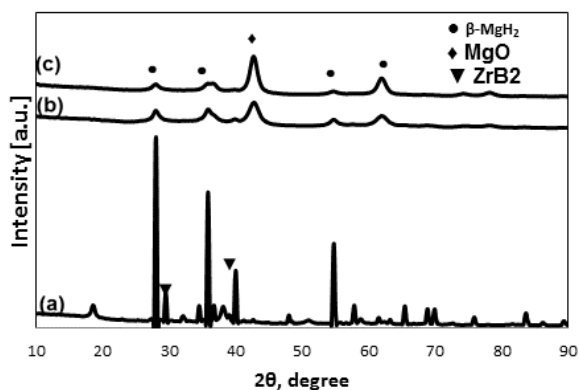

Fig. 4. X-ray diffraction patterns of MgH_2-10 wt% ZrB_2 composite at different milling times: (a) 0 h, (b) 5 h, (c) 30 h.
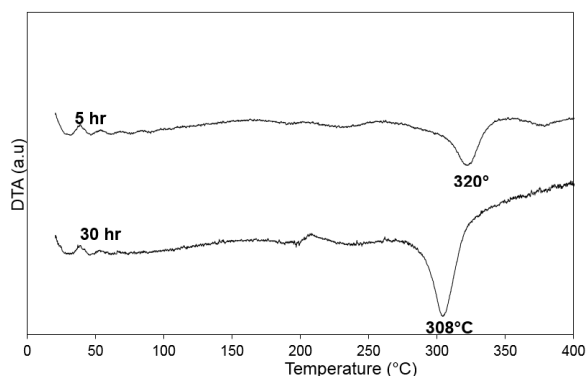

Fig. 5. DTA curves of MgH_2-ZrB_2 composite at selected milling times.

summarized in Table 2. As seen, compared to the mechanically activated MgH_2, a decrease in the dehydrogenation temperature from 319 °C to 308 °C was achieved via co-milling with the ZrB_2 for 30 h.

Fig. 6 shows the morphology of the powder particles at different milling times. After milling time of 5 h, the size of particles decreased significantly and the microstructure is homogeneous (Fig. 6.b). At higher milling time of 30 h, the particles did not undergo any noticeable change, although their size decreased gradually (Fig. 6.c).

Comparison between the mechanically activated MgH_2 with nanocrystalline composite revealed relatively faster particle size refinement in nanocrystalline composite (see Table 2), whereas the average crystallite size of the two samples is not remarkably different. It is known that both the particle size and grain size of magnesium hydride significantly affect its decomposition temperature [13]. It is also reported that mechanical alloying of MgH_2 is accompanied by fracturing as well as clustering and cold welding into large particles. Based on the results obtained in this work, we can deduce that the addition of ZrB_2 powders facilitate the rupture of MgH_2 particles and consequently reduce the particle size [7]. On the other hand, the decrease in the powder particle size can be correlated to a decrease in the hydrogen desorption temperature. Gasan et al. [14] have reported that the crystallite size of powders is not essentially responsible for the decreased hydrogen desorption temperatures of MgH_2, while particle size plays a major role on the hydrogen desorption temperature.

It should be mentioned that the catalytic effect of transition metals belong to two main

Table 2. Average particle size (D), crystallite size (d), lattice strain (ε) and dehydrogenation temperature (T) for MgH_2-10 wt.%ZrB_2 nanocrystalline composite

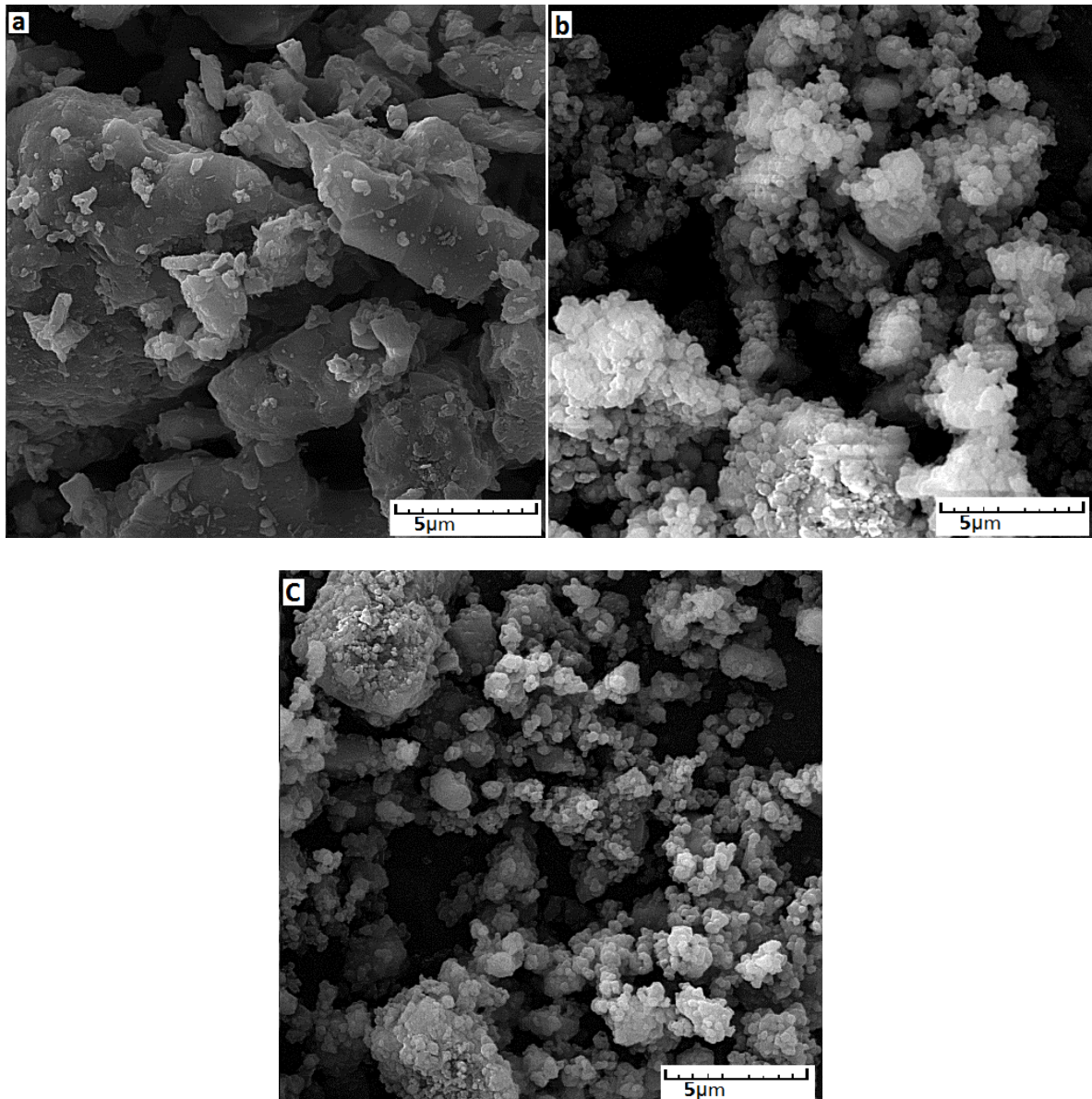| Time,h	Phase	D, μm	d, nm	ε, %	T, (°C)
5	β, MgO	0.8	24	0.5	320
30	β,MgO	0.72	16	0.7	308

Fig. 6. SEM micrographs showing the morphology of MgH$_2$-10 wt% ZrB$_2$ after mechanical alloying for: (a) 0 h, (b) 5 h, and (c) 30 h.

mechanisms: (i) metals (such as Ce, Ti, Nb) forming binary hydrides with a varying stoichiometry which may, at the expense of their hydrogen content, 'pump' hydrogen to the magnesium surface and thus catalyze the dehydrogenation process, and (ii) metals (such as Fe, Co, Cr) forming no binary hydrides, which play the role of active sites on the surface of the magnesium particles and ease the dissociative chemisorption of hydrogen [15]. Based on the XRD results, ternary hydrides are not formed in the Mg-Zr-H and Mg-B-H systems during milling MgH$_2$ with ZrB$_2$ powder. On the other hand, it seems that zirconium and boron play the role of active

sites on the surface of the magnesium particles. Therefore, a change in the rate limiting step from nucleation and growth to phase boundary migration is expected to occur in the presence of transition metals, which can improve dehydrogenation temperature [16].

4. Conclusions

The effect of mechanical milling and ZrB$_2$ addition on the hydrogen desorption temperature of MgH$_2$ was investigated. The following conclusions can be summarized:

- The dehydrogenation of magnesium hydride decreased by mechanical alloying due to particle refinement, formation of

metastable γ-MgH$_2$ phase and finer grain size with accumulation of lattice strain. The lowest dehydrogenation temperature (319 °C) was attained at the 30h mechanical milling.

- The addition of ZrB$_2$ particle to magnesium hydride and mechanical alloying for 30 h reduced the dehydrogenation temperature of magnesium hydride from 319 °C to 308 °C and average particle size of 0.72 μm, which was lower than that of milled MgH$_2$ powder (1.6 μm) at the same condition.

References

1. Sakintuna, B., Lamari-Darkrim, F., Hirscher, M., *Int. J. Hydrogen Energy* Vol. 32 (2007)pp. 1121-1140.
2. Shang, C.X., Bououdina, M., Song, Y., Guo, Z.X., *Int. J. Hydrogen Energy* Vol. 29 (2004)pp. 73-80.
3. Chitsazkhoyi, L., Raygan, S., Pourabdoli, S., *Int. J. Hydrogen Energy* Vol. 38 (2013)pp. 6687-6693.
4. Hao, G., Yunfeng, Z., Liquan, L*., J. Alloys Compd.*Vol. 424 (2006)pp. 382-387.
5. Ranjbar, A., Guo, Z.P., Yu, X.B., Attard, D., Calka, A., Liu, H.K., Int. *J. Hydrogen Energy* Vol. 34 (2009)pp. 7263-7268.
6. Qian, Li., Kuangdi, Xu., Kuochih, Ch.,
7. Milanovic, I., Milosevic, S., Raskovic-Lovre, Z., Novakovic, N., Vujasin, R., Matovic, L., Fernandez, J.F., Sanchez, C., Novakovic, J.G., *Ceram. Int.* Vol. 39 (2013)pp. 4399-4405.
8. Dobrovolsky, V.D., Ershova, O.G., Solonin, Yu.M., Khyzhun, O.Yu., Paul-Boncour, V., *J. Alloys Compd.* Vol. 465 (2008)pp. 177-182.
9. Simchi, H., Kaflou, A., Simchi, A., *Int. J. Hydrogen Energy* Vol. 34 (2009)pp. 7724-7730.
10. Polanski, M., Bystrzycki, J., Plocinski, T., *Int. J. Hydrogen Energy* Vol. 33 (2008)pp. 1859-1867.
11. Varin, A., Czujko, T., Chiu, C., Wronski, Z., *J. Alloys Compd.* Vol. 424 (2006)pp. 356-64.
12. Varin, R., Czujko, T.,Wronski, Z. , *Nanotechnology* Vol. 17 (2006)pp. 3856-65.
13. Gasan, H., Celik, O.N., Aydinbeyli, N., Yaman, Y.M., *Int. J. Hydrogen Energy* Vol. 37 (2012)pp. 1912-1918.
14. Gasan, H., Aydinbeyli, N., Celik, O.N., Yaman, Y.M., *J. Alloys Compd.* Vol. 487 (2009)pp.724-729.
15. Mahmoudi, N., Kaflou, A., Simchi, A., *J. Power Sources* Vol. 196 (2011)pp. 4604-4608.
16. Liang, G., Huot, J., Boily, S., Van Neste, A., Schulz, R., *J. Alloys Compd.* Vol. 292 (1999)pp.247-252.

Xionggang, Lu., Qin, L., *J. Univ. Sci. Technol. B.* Vol.13 (2006)pp. 359-362.